Protonation tuned dipolar order mediated 1H→13C cross-polarization for dissolution-dynamic nuclear polarization experiments

Stuart Elliott, Quentin Stern, Olivier Cala, Sami Jannin

Protonation Tuned Dipolar Order Mediated $^{1}H \rightarrow ^{13}C$ Cross-Polarization for Dissolution-Dynamic Nuclear Polarization Experiments

Stuart J. Elliott[a,b,†], Quentin Stern[a], Olivier Cala[a] and Sami Jannin[a]

[a] Univ. Lyon, CNRS, ENS Lyon, UCBL, Université de Lyon, CRMN UMR 5280, 69100 Villeurbanne, France
[b] Current Address: Department of Chemistry, University of Liverpool, Liverpool L69 7ZD, United Kingdom
[†] Stuart.Elliott@liverpool.ac.uk

Abstract

A strategy of dipolar order mediated nuclear spin polarization transfer has recently been combined with dissolution-dynamic nuclear polarization (*d*DNP) and improved by employing optimized shaped radiofrequency pulses and suitable molecular modifications. In the context of *d*DNP experiments, this offers a promising means of transferring polarization from high-gamma ^{1}H spins to insensitive ^{13}C spins with lower peak power and lower energy compared with state-of-the-art cross-polarization schemes. The role of local molecular groups and the glassing matrix protonation level are both postulated to play a key role in the polarization transfer pathway via an intermediary reservoir of dipolar spin order. To gain appreciation of the mechanisms involved in the dipolar order mediated polarization transfer under *d*DNP conditions, we investigate herein the influence of the pivotal characteristics of the sample makeup: (*i*) revising the protonation level for the constituents of the DNP glass; and (*ii*) utilizing deuterated molecular derivatives. Experimental demonstrations are presented for the case of [1-^{13}C]sodium acetate. We find that the proton sample molarity has a large impact on both the optimal parameters and the performance of the dipolar order mediated cross-polarization sequence, with the ^{13}C signal build-up time drastically shortened in the case of high solvent protonation levels. In the case of a deuterated molecular derivative, we observe that the nearby ^{2}H substituted methyl group is deleterious to the $^{1}H \rightarrow ^{13}C$ transfer phenomenon (particularly at low levels of sample protonation). Overall, increased solvent protonation makes the dipolar order governed polarization transfer significantly faster and more efficient. This study sheds light on the influential sample formulation traits which govern the dipolar order-controlled transfer of polarization and indicates that the polarization transfer efficiencies of deuterated molecules can be boosted and reach high performances simply by adequate solvent protonation.

Keywords: NMR, Hyperpolarization, DNP, *d*DNP, CP, dCP, dipolar order, Protonation

1. Introduction

Traditional nuclear magnetic resonance (NMR) experiments generally engender weak signal outputs due to the low intrinsic sensitivity of nuclear spin ensembles. This limiting factor can be overcome by employing hyperpolarization methodologies such as dissolution-dynamic nuclear polarization (*d*DNP) [1]. This versatile technique has convincingly become a routinely and widely employed approach to boost the detectable polarization from a number of molecules, *e.g.,* such as those of [1-^{13}C]pyruvate, which is relevant to various far-reaching applications in clinical studies performed on human patients [2-4], by up to four orders of magnitude.

*d*DNP yields highly polarized solutions by: (*i*) formulating the *d*DNP sample as a glassy matrix doped with suitable paramagnetic polarizing agents (PAs); (*ii*) freezing the *d*DNP-compatible sample at low-pressure liquid helium temperatures and moderate magnetic fields; (*iii*) irradiating the sample mixture with microwaves; (*iv*) dissolving the sample with a jet of superheated solvent; and (*v*) transferring the sample to a liquid-state NMR spectrometer for signal detection [5]. Stage (*iii*) relies on the transfer of spin polarization from highly polarized electron spins to the weakly polarized nuclear spins of interest. For dilute low-γ nuclear spins at low temperatures, the *d*DNP process typically suffers from excessively long polarization build-up time constants τ_{DNP} sometimes exceeding an hour [6].

Employing radiofrequency (*rf*) pulse sequences which take advantage of the polarization of sensitive nuclear spins such as protons, which polarize rapidly under *d*DNP conditions (typ. 1-3 minutes build-up time constant at temperatures of ~1.0-1.6 K in superfluid helium) [7], can boost the rate of ^{13}C polarization build-ups (by a factor of up to 40) [8-10]. One such sequence is cross-polarization (CP) [11-15], which efficiently transfers ^{1}H polarization to ^{13}C spins in the case that the stringent Hartmann-Hahn matching condition [11], *i.e.,* high B_1-field matching (typ. > 15 kHz to cover the broad ^{1}H NMR linewidth of a static sample) of simultaneously applied ^{1}H and ^{13}C spin-locking *rf*-irradiation during an optimized contact time (typ. > 1 ms), is satisfied. This not only boosts *d*DNP but also provides a way to generate transportable polarized metabolites [16,17].

However, the high *rf*-pulse powers and energies required on the low-gamma spectrometer *rf*-channel often lead to deleterious *rf*-probe arcing in the superfluid helium bath. This detrimental experimental effect limits the scaling up of *d*DNP sample sizes and complicates the implementation of CP for sample volumes surpassing 500 μL, which is imperative for enabling clinical applications using large sample doses [18].

In previous works [19], a dipolar order mediated cross-polarization (dCP) *rf*-pulse sequence was demonstrated to transfer ^{1}H polarization to ^{13}C nuclear spins in static solid-state samples. The polarization transfer *rf*-pulse sequence operates via an intermediary reservoir of dipolar spin order [20-30] and relies on the sequential application of ^{1}H and ^{13}C *rf*-fields, which requires low *rf*-pulse powers and energies, and is therefore more conducive to the hyperpolarization of larger sample volumes under *d*DNP conditions. The efficiency of $^{1}H \rightarrow ^{13}C$ polarization transfer was improved with respect to a state-of-the-art and optimized CP approach by the implementation of shaped *rf*-pulses and molecular derivatives

with favourable properties. However, the exact mechanism of the polarization transfer process for standard DNP-compatible sample formulations requires further elucidation.

In the current Paper, we present the role of molecular and solvent protonation on the dCP polarization transfer mechanism. CP under *d*DNP conditions is usually performed on samples with a protonation extent of ~10-30% [6,8,19]. However, self-glassing *d*DNP-compatible samples such as pyruvic acid have much higher ^{1}H concentrations [31]. It is therefore of interest to investigate whether ^{13}C spins in highly protonated *d*DNP samples can also be hyperpolarized by dCP in an efficient manner. Furthermore, there has been recent interest in transferring the high levels of ^{1}H polarization to ^{13}C spins in deuterated molecules since such systems often display significantly longer ^{13}C relaxation time constants in solution after dissolution [32]. CP experiments performed on deuterated molecules have been shown to work equally as well as compared to their protonated counterparts [32], despite slower transfer dynamics. It is additionally worth considering if the ^{1}H→^{13}C polarization transfer works as well in the case of dCP for deuterated molecular systems.

In the context of our *d*DNP experiments, we introduce the following sample formulation modifications with respect to conventional *d*DNP sample constituents: (*i*) increasing the protonation extent of the DNP solvent; and (*ii*) employing deuterated molecular candidates. We report experimental observations for [1-^{13}C]sodium acetate and its methyl deuterated derivative for a variety of solvent protonation extents. The ^{1}H sample molarity was shown to significantly influence the parameters and performance efficiency of the dCP *rf*-pulse sequence, *e.g.,* the optimal ^{1}H→^{13}C dCP nuclear polarization transfer time was drastically reduced at high levels of solvent protonation. It was also found that deuterated molecular moieties reduce the efficiency of the dCP transfer process, with deleterious effects observed for the build-up of the ^{13}C NMR signal in certain cases, *i.e.*, low extents of sample protonation.

2. Methods

2.1. Sample Preparation

Table 1: ^{1}H solvent protonation percentages $h_{X\%}$, ^{1}H sample molarities [H] and relative proportions of H_2O/D_2O/glycerol-h_8/glycerol-d_8 used for the DNP solvent matrices of the samples employed in this study.

	Samples					
	I				**II**	
$h_{X\%}$	10	40	70	100	10	100
[H] / M	20.07	53.38	87.49	119.70	11.07	110.70
H_2O	1	4	4	4	1	4
D_2O	3	0	0	0	3	0
glycerol-h_8	0	0	3	6	0	6
glycerol-d_8	6	6	3	0	6	0

Solutions of 3 M [1-^{13}C]sodium acetate (**I**) and [1-^{13}C]sodium acetate-d_3 (**II**) doped with 50 mM TEMPOL radical (all compounds purchased from *Sigma Aldrich*) were prepared in the glass-forming mixtures of H_2O/D_2O/glycerol-h_8/glycerol-d_8 (*v*/*v*/*v*/*v*) given in Table 1. All samples were sonicated for ~10 minutes. Paramagnetic TEMPOL radicals were chosen to polarize ^{1}H spins most efficiently under our *d*DNP conditions.

2.2. Sample Freezing

100 μL volumes of each sample were separately pipetted into a Kel-F sample cup and rapidly immersed in the liquid helium bath of a 7.05 T prototype *Bruker Biospin* polarizer equipped with a specialized *d*DNP probe and running *TopSpin 3.5* software. The sample temperature was further reduced to 1.2 K by adjusting the pressure of the variable temperature insert (VTI) towards ~0.7 mbar.

2.3. Dynamic Nuclear Polarization

The samples were polarized by applying microwave irradiation at $f_{\mu w}$ = 197.648 GHz (positive lobe of the DNP spectrum) with triangular frequency modulation of amplitude $\Delta f_{\mu w}$ = 120 MHz [33] and rate f_{mod} = 0.5 kHz at a power of ca. 100 mW at the output of the microwave source and ca. 30 mW reaching the DNP cavity [34] which were optimized by using sample $\mathbf{I}_{10\%}$ prior to commencing experiments to achieve the highest possible ^{1}H polarization.

2.4. Microwave Gating

Microwave gating was employed shortly before and during *d*DNP polarization transfer experiments (see Section 2.5) to allow the electron spin ensemble to return to a highly polarized state, which happens on the timescale of the longitudinal electron relaxation time constant (typ. T_{1e} = 100 ms with P_e = 99.93% under our experimental *d*DNP conditions) [35]. Microwave gating therefore affords a means to substantially reduce paramagnetic relaxation, and as a result; the ^{1}H and ^{13}C relaxation time constants in the presence of an *rf*-field ($T_{1\rho}$) are extended by orders of magnitude, allowing spin-locking *rf*-pulses to be much longer, and ultimately significantly increasing the overall efficiency of nuclear spin polarization transfer.

2.5. dCP RF-Pulse Sequence

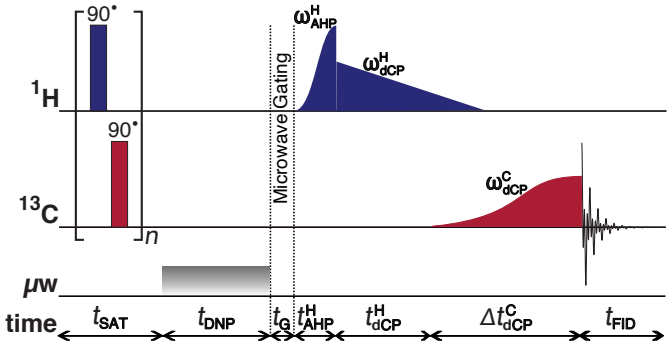

Figure 1: Schematic representation of the dCP *rf*-pulse sequence used for preparing dipolar order in samples **I** and **II** and monitoring its conversion to ^{13}C magnetization. The experiments used the following parameters, chosen to maximize the efficiency of the dCP *rf*-pulse sequence: n = 50; t_{DNP} = 5 s; t_G = 0.5 s; $\omega^{H}_{AHP}/2\pi$ = 27.8 kHz; t^{H}_{AHP} = 175 μs; $\omega^{H}_{dCP}/2\pi$ = 16.9 kHz; t^{H}_{dCP} = 475 μs; $\omega^{C}_{dCP}/2\pi$ = 14.6 kHz. AHP = adiabatic half-passage. AHP sweep width = 100 kHz. The $\pi/2$ saturation *rf*-pulses use a thirteen-step phase cycle to remove residual magnetization at the beginning of each experiment: {0, π/18, 5π/18, π/2, 4π/9, 5π/18, 8π/9, π, 10π/9, 13π/9, π/18, 5π/3, 35π/18}. The resonance offset was placed at the centre of the ^{1}H and ^{13}C NMR peaks.

In previous studies [19,36,37], variants of the dipolar order mediated cross-polarization (dCP) *rf*-pulse sequence which included shaped *rf*-pulses were found to have improved ^{1}H→^{13}C nuclear polarization transfer efficiencies versus the original non-Zeeman polarization transfer (NZPT) experiment

proposed by Vieth and Yannoni [19,21] from which our work was inspired. Figure 1 shows this sequence adapted for our *d*DNP experiments.

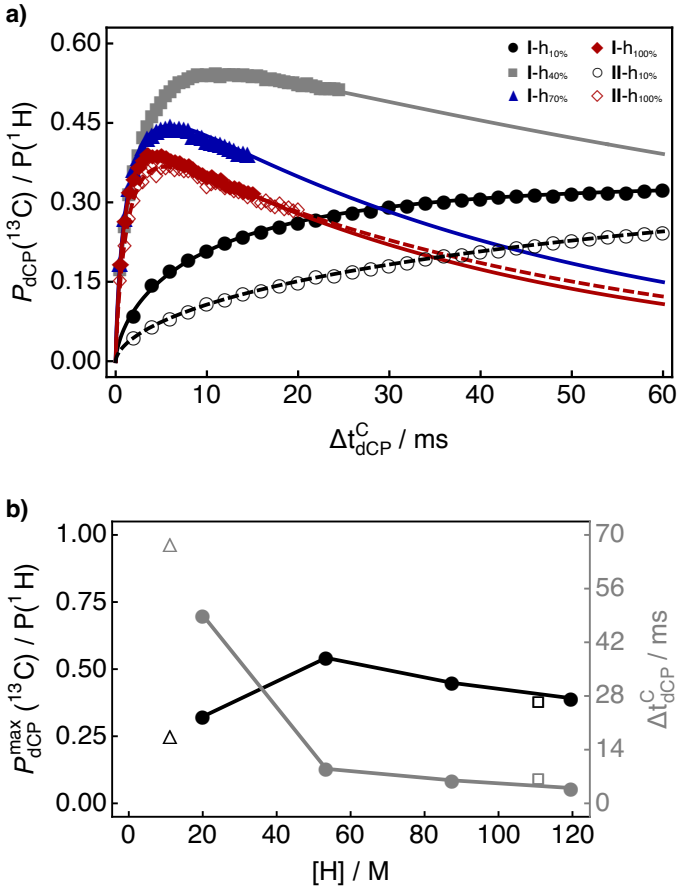

Figure 2: a) ^{13}C polarizations normalized by ^{1}H polarizations $P_{dCP}(^{13}C)/P(^{1}H)$ as a function of the ^{13}C dCP *rf*-pulse duration Δt^{C}_{dCP} acquired at 7.05 T (^{1}H nuclear Larmor frequency = 300.13 MHz, ^{13}C nuclear Larmor frequency = 75.47 MHz) and 1.2 K. The data presented in (a) were acquired by using the dCP *rf*-pulse sequence shown in Figure 1. Solid and dashed lines correspond to best fits of the filled and open data points, respectively, and have the following fitting function: $A(1-\exp\{-(R^{C}_{dCP}t)^{\beta}\}\exp\{-R^{C}_{relax}t\})$. b) ^{13}C polarizations normalized by ^{1}H polarizations $P^{max}_{dCP}(^{13}C)/P(^{1}H)$ (black) and ^{13}C dCP *rf*-pulse durations Δt^{C}_{dCP} (grey) as a function of the ^{1}H sample molarity [H] (same experimental *d*DNP conditions as in a)). Filled symbols: Sample **I**; and open symbols: Sample **II**. The values for the open triangles have been adjusted (see the ESI for more details) to compensate for the non-plateauing behaviour of the ^{13}C build-up curve for sample **II**-h$_{10\%}$ (shown in a)).

The dCP *rf*-pulse sequence operates as follows:

(*i*) a saturation sequence of 90° *rf*-pulses with alternating phases separated by a short delay repeated *n* times (typ. *n* = 50) kills residual magnetization from previous experiments on both *rf*-channels;

(*ii*) the microwave source becomes active for a time t_{DNP} during which ^{1}H DNP builds-up;

(*iii*) the microwave source is deactivated, and a delay of duration t_G = 0.5 s occurs before the next step, thus permitting the electron spins to relax to their highly polarized thermal equilibrium state [35];

(*iv*) a preparatory ^{1}H adiabatic half-passage (AHP) *rf*-pulse creates transverse ^{1}H magnetization;

(*v*) a linearly decreasing ramp ^{1}H dCP *rf*-pulse of amplitude ω^{H}_{dCP} and length t^{H}_{dCP} prepares proton dipolar order;

(*vi*) an increasing hyperbolic tangent ^{13}C dCP *rf*-pulse of amplitude ω^{C}_{dCP} and length Δt^{C}_{dCP} presumably converts the ^{1}H-^{1}H dipolar order into ^{13}C magnetization;

(*vii*) the induced ^{13}C NMR signal is detected.

Further details regarding dCP *rf*-pulse sequence operation are given elsewhere [19].

3. Results

3.1. Dipolar Order Mediated Cross-Polarization

The build-up of ^{13}C polarizations normalized by the corresponding ^{1}H polarizations $P_{dCP}(^{13}C)/P(^{1}H)$ as a function the ^{13}C dCP *rf*-pulse duration Δt^{C}_{dCP} was monitored by using the dCP *rf*-pulse sequence depicted in Figure 1. The dCP *rf*-pulse sequence was repeated with incremented values of the ^{13}C dCP *rf*-pulse duration Δt^{C}_{dCP}, with all other *rf*-pulse parameters fixed. Experiments were performed after only 5 s of DNP to minimize the effects of radiation damping on the quantification of the ^{1}H polarization [38,39].

The influence of the ^{13}C dCP *rf*-pulse duration Δt^{C}_{dCP} on the build-up of the normalized ^{13}C polarizations for several samples is shown in Figure 2a. Experimental values lie between 0 (no transfer) and 1 (theoretical maximum). The influence of the ^{1}H sample molarity on the other properties of the ^{1}H and ^{13}C dCP *rf*-pulses, *e.g.,* peak *rf*-power, was found to be minimal.

For samples with low ^{1}H molarities, the normalized ^{13}C polarization build-up curves plateau at long values of the ^{13}C dCP *rf*-pulse duration (Δt^{C}_{dCP} > 40 ms). Samples with increased ^{1}H molarities, *i.e.,* for sample protonation levels ≥ 40%, the normalized ^{13}C polarization build-up curves feature maxima at relatively short values of the ^{13}C dCP *rf*-pulse duration (Δt^{C}_{dCP} < 15 ms), followed by a slowly decaying component.

The ^{13}C/^{1}H polarization ratio $P_{dCP}(^{13}C)/P(^{1}H)$ allows a direct comparison of the dCP transfer efficiency for samples with proton spins which polarize to different extents. The quantity $P^{max}_{dCP}(^{13}C)/P(^{1}H)$ is plotted in Figure 2b (black data points and axis) as the normalized ^{13}C polarization maxima from the curves shown in Figure 2a as a function of the ^{1}H sample molarity [H] for all the samples employed in this study. The open symbols correspond to samples: **II**-h$_{10\%}$ (open triangle); and **II**-h$_{100\%}$ (open square). $P^{max}_{dCP}(^{13}C)/P(^{1}H)$ increases with an increasing ^{1}H sample molarity, until a maximum is reached at ~53 M, after which the polarization ratio decreases with a further increase in the ^{1}H sample molarity. The methyl deuterated molecular derivative additionally fits this trend.

The durations of the ^{13}C dCP *rf*-pulses Δt^{C}_{dCP} at the normalized ^{13}C polarization maxima for the curves presented in Figure 2a are shown by the grey data points and axis in Figure 2b. The filled circles correspond to sample **I** for various ^{1}H sample molarities [H], and these data points are connected via the grey line. There is a general trend, for all samples, of decreasing ^{13}C dCP *rf*-pulse durations Δt^{C}_{dCP} with increasing ^{1}H sample molarities, with a rapid decrease at relatively low ^{1}H sample molarities. This curve begins to plateau at relatively high ^{1}H sample molarities (exceeding ~60 M). Even though the open symbols belong to a different molecular spin system, the data points still fit the overall trend.

The build-ups of the normalized ^{13}C polarizations were found to have strong stretched exponential behaviours in all cases. The experimental data in Figure 2a are well fitted with a phenomenological stretched exponential function using two rate constants denoted R^{C}_{dCP} and R^{C}_{relax} responsible for the build-up and decay of the normalized ^{13}C polarizations, respectively. Stretched exponential function: $A(1-\exp\{-(R^{C}_{dCP}t)^{\beta}\})\exp\{-R^{C}_{relax}t\}$, where A is a fitting constant, R^{C}_{dCP} =

$R^*_{\mathrm{dCP}}\Gamma(1/\beta)/\beta$, R^*_{dCP} is the average ^{13}C build-up rate constant, β is the breadth of the distribution of ^{13}C build-up rate constants and $\Gamma(1/\beta)$ is the gamma function (see the Electronic Supporting Information (ESI) for more details). We attribute the average ^{13}C build-up rate constants R^*_{dCP} to be ones associated with the generation of the normalized ^{13}C polarizations. It should be noted that R^{C}_{relax} is an "apparent" relaxation rate constant. The connection between the ^{13}C spin bath and the lattice is indirect, likely via the ^{1}H spins.

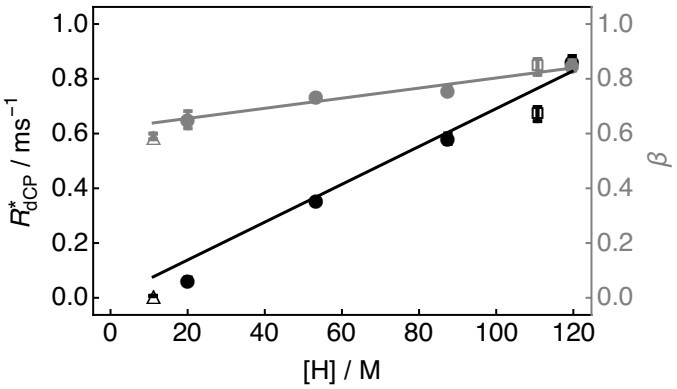

Figure 3: Average ^{13}C dCP *rf*-pulse build-up rate constants R^*_{dCP} (black) and breadths of the distributions of the ^{13}C build-up rate constants β (grey) as a function of the ^{1}H sample molarity [H] acquired at 7.05 T (^{1}H nuclear Larmor frequency = 300.13 MHz, ^{13}C nuclear Larmor frequency = 75.47 MHz) and 1.2 K. The filled symbols were fitted with a straight-line function including an intercept: $y = m_y \times [\mathrm{H}] + a_y$. Best fit values: $y = R^*_{dCP}$: $m_{R^*_{dCP}}$ = 0.007 M^{-1}ms^{-1}; $a_{R^*_{dCP}}$ = 0 ms^{-1} (forced); $y = \beta$: m_β = 0.002 M^{-1}; a_β = 0.6. Filled symbols: Sample **I**; and open symbols: Sample **II**. In some cases, the error bars are smaller than the data points.

From fitting the normalized ^{13}C polarizations as a function of the ^{13}C dCP *rf*-pulse durations $\Delta t^{\mathrm{C}}_{dCP}$ rate constants for the build-up and decay of the normalized ^{13}C polarizations, namely R^*_{dCP} and R^{C}_{relax}, respectively, and the breadths of the distributions of ^{13}C build-up rate constants β, can be estimated. The value of the average ^{13}C build-up rate constant R^*_{dCP} for the experimental curves presented in Figure 2a are shown by the black data points and axis in Figure 3. There is an overall trend of a linearly increasing value of R^*_{dCP} with an increasing ^{1}H sample molarity [H]. The data points for the methyl deuterated molecular analogue also follow this trend even though the local molecular moiety lacks any considerable degree of protonation. A similar trend is observed for R^{C}_{relax} (see the ESI for more details).

The breadths of the distributions of ^{13}C build-up rate constants β for the experimental curves presented in Figure 2a are shown by the grey data points and axis in Figure 3. β increases linearly with an increasing ^{1}H sample molarity [H]. The data points for the methyl deuterated molecular candidate also follow this trend, with the value of β almost identical for the two most highly protonated samples.

Straight-line fits to the filled symbols presented in Figure 3 are indicated by the solid lines. The experimental data are well fitted with relationships of the kind: $y([\mathrm{H}]) = m_y \times [\mathrm{H}] + a_y$; where $y([\mathrm{H}])$ is either R^*_{dCP} or β, m_y is the slope of the straight-line fit, [H] is the ^{1}H sample molarity and a_y is the intercept. See the caption of Figure 3 for best fit values. The intercept a_β was forced to zero in the case of R^*_{dCP}. The experimental data points from the open symbols (sample **II**) approximately follow the trend of the filled symbols (sample **I**).

3.2. Cross-Polarization

The performance efficiency of the dCP *rf*-pulse sequence was compared with a traditional CP experiment [8-15], which is described in the ESI along with an *rf*-pulse sequence diagram and all optimized parameters. To compare the ^{13}C polarizations achieved for each sample after a single CP contact with those obtained by implementing the dCP *rf*-pulse sequence with a sole ^{1}H→^{13}C polarization transfer step, experiments employed 600 s of direct ^{1}H DNP at 1.2 K prior to polarization transfer to the ^{13}C heteronucleus. The ^{13}C polarization level $P_{\mathrm{dCP}}(^{13}\mathrm{C})$ obtained as a result of using the dCP *rf*-pulse sequence is calculated by scaling $P_{\mathrm{CP}}(^{13}\mathrm{C})$ (the analogous quantity for the CP experiment) by a factor of $I_{\mathrm{dCP}}/I_{\mathrm{CP}}$.

Table 2: ^{13}C nuclear spin polarization levels $P_{\mathrm{dCP}}(^{13}\mathrm{C})$ and $P_{\mathrm{CP}}(^{13}\mathrm{C})$ measured after 10 minutes of DNP for the ^{1}H depleted and enriched samples (**I** and **II**) employed in this study amassed by using the dCP and CP *rf*-pulse sequences, respectively, acquired at 7.05 T (^{1}H nuclear Larmor frequency = 300.13 MHz, ^{13}C nuclear Larmor frequency = 75.47 MHz) and 1.2 K.

	Samples			
	I-h$_{10\%}$	**II**-h$_{10\%}$	**I**-h$_{100\%}$	**II**-h$_{100\%}$
$P_{\mathrm{dCP}}(^{13}\mathrm{C})$ / %	19.0	15.0	14.3	12.8
$P_{\mathrm{CP}}(^{13}\mathrm{C})$ / %	37.3	44.6	23.7	19.7

For sample **I**-h$_{10\%}$, ^{13}C spin polarizations of $P_{\mathrm{dCP}}(^{13}\mathrm{C})$ = 19.0% and $P_{\mathrm{CP}}(^{13}\mathrm{C})$ = 37.3% were measured by using the dCP and CP *rf*-pulse sequences, respectively. This is reasonably similar to those of the methyl deuterated molecular derivative (sample **II**-h$_{10\%}$): $P_{\mathrm{dCP}}(^{13}\mathrm{C})$ = 15.0% and $P_{\mathrm{CP}}(^{13}\mathrm{C})$ = 44.6%. These results (see Table 2) are in approximate agreement with a previous study [32]. ^{13}C polarization levels higher than 60% are anticipated by using a multiple CP contact approach [8-16].

In the case of the heavily protonated sample formulations, sample **I**-h$_{100\%}$ records significantly lower ^{13}C nuclear spin polarizations than sample **I**-h$_{10\%}$ (see Table 2) under the same experimental *d*DNP conditions: $P_{\mathrm{dCP}}(^{13}\mathrm{C})$ = 14.3% and $P_{\mathrm{CP}}(^{13}\mathrm{C})$ = 23.7%. The same is also true for the methyl deuterated molecular analogue (samples **II**-h$_{10\%}$ and **II**-h$_{100\%}$): $P_{\mathrm{dCP}}(^{13}\mathrm{C})$ = 12.8% and $P_{\mathrm{CP}}(^{13}\mathrm{C})$ = 19.7%. It is important to indicate that a plateau in the ^{1}H polarization of this sample has likely not been reached after 10 minutes of ^{1}H DNP, and that the ^{1}H spins in this sample are expected to continue polarizing. However, the plateau in ^{1}H polarization is lower compared with samples which have reduced proton concentrations, and therefore the performances of fully protonated samples are anticipated to remain lower than those of their partially protonated counterparts (even if a ^{1}H polarization plateau is achieved). The ^{1}H DNP build-up is also slower, in this case, since the sample of interest contains more ^{1}H spins to polarize per electron spin.

It is also worth noting that the contact CP *rf*-pulse durations are significantly reduced, by a factor of ~3.4 ± 0.05, when fully protonated DNP samples are used, compared with those of ~10% protonation extent. For example, the optimal contact *rf*-pulse duration for sample **II**-h$_{10\%}$ is 9.5 ms, whilst for sample **II**-h$_{100\%}$ the duration of the contact CP *rf*-pulse is 2.75 ms. These results also suggest that the role of DNP solvent protonation plays an important part regarding the dynamics of CP. However, the relative reduction in the ^{13}C *rf*-pulse duration for CP is much less than in the case of dCP.

4. Discussion

4.1 ^{13}C Polarization Build-Up

The profiles of the ^{13}C build-up curves in Figure 2a have remarkably different forms depending on the protonation extent of the DNP solvent. At low ^{1}H sample molarities, the ^{13}C build-up curves increase towards an eventual plateau, whilst at high ^{1}H sample molarities, the ^{13}C build-up curves peak at a maximum before decaying towards a reduced signal intensity on a longer time scale. The stretched exponential model fit implies that the dCP polarization transfer is governed by the ^{1}H-^{13}C internuclear separation. This is ultimately responsible for the initial build-up and gradual decay of the experimental profiles presented in Figure 2a. The initial build-up components of the curves belonging to the higher ^{1}H sample molarities are related to decreased ^{1}H-^{13}C internuclear separations, whilst the decaying components of these curves are likely attributable to increased dipolar relaxation between ^{1}H and ^{13}C spins.

The polarization ratio $P_{\mathrm{dCP}}^{\mathrm{max}}(^{13}\mathrm{C})/P(^{1}\mathrm{H})$ reaches a maximum at a ~53 M proton sample molarity, where the dCP pulse sequence transfers ~54% of the original ^{1}H polarization $P(^{1}\mathrm{H})$ to the ^{13}C nuclear site. This result indicates that there is a delicate balance in the ^{1}H solvent protonation extent, which is likely a trade-off between improved polarization transfer rates and $T_{1\rho}$ relaxation, and that a reasonable quantity of proton spins (~40%) are required to make the dCP *rf*-pulse sequence suitably efficient (see Figure 2b), albeit with reduced ^{1}H DNP efficiencies at increased ^{1}H molarities. Given that samples **I**-h$_{70\%}$ and **I**-h$_{100\%}$ achieve higher ratios of $P_{\mathrm{dCP}}^{\mathrm{max}}(^{13}\mathrm{C})/P(^{1}\mathrm{H})$ compared with sample **I**-h$_{10\%}$, it is apparent that increasing the ^{1}H bath concentration, and consequently improving the dCP transfer process, outweighs the associated costs of increased proton induced $T_{1\rho}$ relaxation.

4.2 dCP Transfer Efficiency vs. Protonation

Figure 2b (grey data points and axis) shows a sharp decrease in the ^{13}C dCP *rf*-pulse optimal duration $\Delta t_{d\mathrm{CP}}^{\mathrm{C}}$ as a function of the ^{1}H sample molarity [H]. This trend indicates that the $^{1}\mathrm{H}\rightarrow{}^{13}\mathrm{C}$ polarization conversion becomes increasingly more efficient once the sample has a sufficient ^{1}H solvent molarity (see the ESI for more details).

At a 100% sample protonation level, *i.e.,* a ^{1}H sample molarity of ~120 M, the distances between neighbouring ^{1}H nuclear spins in the DNP solvent are reduced by a factor of ~2.15 with respect to a sample of 10% solvent protonation ([H] $\simeq$ 20 M), which increases the ^{1}H-^{1}H dipolar couplings ω_{HH} by a factor of ~10. Such a relationship assumes that the dipolar couplings are proportional to the ^{1}H sample concentration [H], since ω_{HH} is proportional to the inverse cube of the ^{1}H-^{1}H distance, which is itself proportional to the inverse cube of the concentration. The same is true for the ^{1}H-^{13}C internuclear separations, and their respective dipolar couplings ω_{HC}. If the transfer of $^{1}\mathrm{H}\rightarrow{}^{13}\mathrm{C}$ polarization is governed by such dipolar interactions, then it is permissible that the ^{13}C dCP *rf*-pulse duration $\Delta t_{d\mathrm{CP}}^{\mathrm{C}}$ is inversely proportional to these dipolar couplings. Since a precise relationship between ω_{HH}, ω_{HC} and $\Delta t_{d\mathrm{CP}}^{\mathrm{C}}$ is not yet known, this hypothesis can be tested by considering the ratio of $\Delta t_{d\mathrm{CP}}^{\mathrm{C}}$ at 10% and 100% ^{1}H sample protonations, which for sample **I** is ~8.2. In the case of sample **II**, the ratio of $\Delta t_{d\mathrm{CP}}^{\mathrm{C}}$ at 10% and 100% ^{1}H sample protonations is ~11.3. These results suggest that the methyl group moiety local to the ^{13}C labelled nuclear site plays an important role in the transfer of polarization from ^{1}H to ^{13}C spins. This could be the reason for the reduced dCP *rf*-pulse sequence performance for sample **II**-h$_{10\%}$ (see the ESI for more details).

4.3 Dipolar Order in the Sample Bulk

The ^{13}C nuclear site in sample **II**-h$_{10\%}$ was able to polarize to a reasonable degree without any attached protons (see Figure 2a). However, there are still a non-negligible number of proton spins within this sample due to the protonation of the DNP juice used in our experiments. These results therefore suggest that proton dipolar order is mostly generated between ^{1}H spins in the DNP sample solvent (or between the solvent and the molecule of interest) by the ^{1}H dCP *rf*-pulse, and subsequently transferred from the solvent ^{1}H spins to the ^{13}C spins of interest via the ^{13}C dCP *rf*-pulse. As a result, the average ^{13}C dCP *rf*-pulse build-up rate constant $R_{d\mathrm{CP}}^{*}$ for sample **II**-h$_{10\%}$ is likely to indicate the rate of $^{1}\mathrm{H}\rightarrow{}^{13}\mathrm{C}$ polarization transfer mediated by proton dipolar order generated within the DNP matrix itself and provides a minimum value of $R_{d\mathrm{CP}}^{*}$ for potential future samples. The smaller average ^{13}C dCP *rf*-pulse build-up rate constant $R_{d\mathrm{CP}}^{*}$ for sample **II**-h$_{10\%}$ compared with sample **I**-h$_{10\%}$ is likely due to increased internuclear separations between ^{1}H spins participating in the proton dipolar order within the solvent and the target ^{13}C nucleus of the molecule of interest due to the inclusion of the deuterated methyl group. Without such an effect, it is unlikely that the ^{13}C nuclear site in sample **II**-h$_{10\%}$ would polarize as efficiently.

In Figure 3 it was observed that the average ^{13}C dCP *rf*-pulse build-up rate constants $R_{\mathrm{dCP}}^{\mathrm{C}}$ increase linearly with the ^{1}H sample molarity. The reason for this trend is likely to be similar to that observed for the ^{13}C dCP *rf*-pulse duration $\Delta t_{d\mathrm{CP}}^{\mathrm{C}}$ with ^{1}H sample molarity. At high ^{1}H sample molarities ([H] > 100 M), the ^{13}C dCP *rf*-pulse build-up rate $R_{\mathrm{dCP}}^{\mathrm{C}}$ for sample **I**-h$_{100\%}$ is a factor of ~1.26 greater than for sample **II**-h$_{100\%}$. At low ^{1}H sample molarities ([H] $\lesssim$ 20 M), the ^{13}C dCP *rf*-pulse build-up rate R_{dCP}^{*} for sample **I**-h$_{10\%}$ is a factor of ~9 greater than for sample **II**-h$_{10\%}$. This indicates that although the $^{1}\mathrm{H}\rightarrow{}^{13}\mathrm{C}$ dCP polarization transfer mechanism is mostly operating via the proton spins embedded within the DNP solvent at high ^{1}H molarities, given that sample **II**-h$_{100\%}$ has no directly bound ^{1}H spins, the local methyl moiety plays a more pivotal role in the $^{1}\mathrm{H}\rightarrow{}^{13}\mathrm{C}$ dCP transfer of polarization to the ^{13}C nuclear spin at low levels of sample protonation.

The breadths of the distributions of ^{13}C build-up rate constants β were shown to increase with an increasing ^{1}H sample molarity [H], see Figure 3 (grey data points and axis). This indicates that as [H] increases the average ^{13}C build-up rate constants $R_{d\mathrm{CP}}^{*}$ converge towards a sole value. The value of β for the ^{2}H substituted molecular system is almost identical to that of its protonated counterpart at high levels of sample protonation. This result suggests that there is a very similar distribution of average ^{13}C dCP *rf*-pulse build-up rates R_{dCP}^{*} for both samples, which again indicates that the ^{1}H spins within the DNP solvent are mostly responsible for the $^{1}\mathrm{H}\rightarrow{}^{13}\mathrm{C}$ dCP transfer of polarization at increased levels of sample protonation.

A discussion regarding effective dCP polarization transfer rates, *i.e.*, the dCP polarization transfer rate per unit of proton spin concentration, is given in the ESI.

4.4 Hyperpolarization of deuterated molecules

The observed ^{13}C polarization level (after 10 minutes of DNP) for sample **II**, *i.e.,* the methyl deuterated molecular system, is lower by a factor of ~1.27 compared with that of

sample **I** in the case of low levels of ^{1}H sample molarity (see Table 2). However, the results shown in Figure 3 and the ESI indicate that the dCP *rf*-pulse sequence relies on a pool of proton dipolar spin order which is contained between the proton spins within the DNP solvent. This claim is supported by considering that when the solvent ^{1}H molarity is increased from 10%→100% for sample **I**, R^{*}_{dCP} increases by a factor of ~10.3. The same modification in solvent protonation extent for sample **II** leads to an increase in R^{*}_{dCP} by a factor of ~74. These results highlight the beneficial role of protonating the DNP solvent in the case of deuterated molecular systems, with the performance efficiency of sample **II**-$h_{10\%}$ significantly improved by increasing the protonation level of the DNP solvent (see Table 2 and the ESI). However, the overall level of ^{13}C polarization is reduced (even after 5 s of DNP and microwave gating) in the case of highly protonated samples, given the longer ^{1}H polarization build-up timescales associated with these samples.

Previous investigations regarding the overall performance of CP-based *rf*-methods on deuterated derivatives of ^{13}C-labelled small molecules has demonstrated that the level of molecular deuteration has a negligible effect on the efficiency of various CP approaches, since proton Zeeman order within the bulk of the DNP glassing matrix is employed for the polarization transfer process [32]. These results are clearly replicated for the dCP *rf*-pulse sequence and imply that ^{2}H substituted molecules can be polarized to the nearly same extent as their protonated counterparts by using the dCP *rf*-pulse sequence at increased levels of sample protonation. Clearly, an increased level of overall sample protonation was found to have a positive impact on the dCP *rf*-pulse sequence relative to the performance of the CP *rf*-pulse sequence, which experienced a much more dramatic decrease in ^{13}C polarization with increasing sample protonation for both protonated and deuterated molecular derivatives (see Table 2), although there is less ^{1}H polarization available for dCP/CP transfer per unit DNP time.

The ^{1}H (and ^{13}C) NMR linewidths were found to increase with an increasing ^{1}H sample molarity, as shown in the ESI, which may also have consequences regarding the performances of the dCP and CP *rf*-pulse sequences.

5. Conclusions

We have shown the importance of molecular and solvent protonation on the ^{1}H→^{13}C transfer mechanism of nuclear spin polarization in the case of a dCP *rf*-pulse sequence which employs an intermediary reservoir of dipolar spin order. The importance of each protonated component was demonstrated by investigating the following sample formulation strategies: (*i*) modifying the protonation extent of the DNP solvent; and (*ii*) utilizing methyl deuterated molecular targets. The overall ^{1}H sample molarity was found to have a significant influence on both the optimal parameters and efficiency of the dCP *rf*-pulse sequence, and in general made the approach substantially shorter in duration and more efficient. The absence of ^{1}H nuclear spins in ^{2}H labelled molecular moieties, *e.g.,* methyl groups, proximal to the ^{13}C sites of interest were found to be detrimental to the ^{1}H→^{13}C transfer process and decrease the dCP transfer rate of the ^{13}C signal build-up (particularly at low ^{1}H sample molarities).

This investigation has provided insights into the key sample formulation characteristics which control the dipolar order mediated transfer of ^{1}H polarization to ^{13}C nuclear spins and indicates that the dCP polarization transfer efficiencies of deuterated molecular candidates can be improved by increasing the protonation of the DNP solvent matrix. The large excess of ^{1}H spins within the DNP glassing matrix means that ^{13}C spins in a wide variety of molecular systems can be easily polarized by a low peak power and energy *rf*-pulse sequence which is straightforward to implement and robust with respect *rf*-pulse parameter optimization. Such molecular systems include deuterated molecules, dilute samples or molecules of interest with ^{13}C sites at natural abundance. A raft of numerical simulations could be employed to elucidate the nature of the polarization transfer mechanism in such cases. These results are encouraging for the future usage of the dCP *rf*-pulse sequence, which may be advantageous for certain applications that require reduced peak *rf*-power requirements and forge a path towards hyperpolarization experiments compatible with increased sample volumes, *e.g.,* such as those implemented in clinical research.

Acknowledgements

This research was supported by ENS-Lyon, the French CNRS, Lyon 1 University, the European Research Council under the European Union's Horizon 2020 research and innovation program (ERC Grant Agreements No. 714519 / HP4all and Marie Skłodowska-Curie Grant Agreement No. 766402 / ZULF). The authors gratefully acknowledge *Bruker Biospin* for providing the prototype *d*DNP polarizer, and particularly Dmitry Eshchenko, Roberto Melzi, Marc Rossire, Marco Sacher and James Kempf for scientific and technical support. The authors additionally acknowledge Gerd Buntkowsky (Technische Universitat Darmstadt) who kindly communicated data associated with prior publications to us; Burkhard Luy (Karlsruhe Institute of Technology) for enlightening discussions; Catherine Jose and Christophe Pages for use of the ISA Prototype Service; Stéphane Martinez of the UCBL mechanical workshop for machining parts of the experimental apparatus; and Samuel Cousin and Morgan Ceillier for maintaining the experimental setup.

References

[1] J. H. Ardenkjær-Larsen, B. Fridlund, A. Gram, G. Hansson, L. Hansson, M. H. Lerche, R. Servin, M. Thaning and K. Golman, *Proc. Natl. Acad. Sci.*, **2003**, 100, 10158-10163.

[2] S. J. Nelson, J. Kurhanewicz, D. B. Vigneron, P. E. Z. Larson, A. L. Harzstark, M. Ferrone, M. van Criekinge, J. W. Chang, R. Bok, I. Park, G. Reed, L. Carvajal, E. J. Small, P. Munster, V. K. Weinberg, J. H. Ardenkjær-Larsen, A. P. Chen, R. E. Hurd, L.-I. Odegardstuen, F. J. Robb, J. Tropp and J. A. Murray, *Sci. Transl. Med.*, **2013**, 5, 198.

[3] H.-Y. Chen, R. Aggarwal, R. A. Bok, M. A. Ohliger, Z. Zhu, P. Lee, J. W. Goodman, M. van Criekinge, L. Carvajal, J. B. Slater, P. E. Z. Larson, E. J. Small, J. Kurhanewicz and D. B. Vigeron, *Prostate Cancer Prostatic Dis.*, **2020**, 23, 269-276.

[4] F. A. Gallagher, R. Woitek, M. A. McLean, A. B. Gill, R. M. Garcia, E. Provenzano, F. Reimer, J. Kaggie, A. Chhabra, S. Ursprung, J. T. Grist, C. J. Daniels, F. Zaccagna, M.-C. Laurent, M. Locke, S. Hilborne, A. Frary, T. Torheim, C. Boursnell, A. Schiller, I. Patterson, R. Slough, B. Carmo, J. Kane, H. Biggs, E. Harrison, S. S. Deen, A. Patterson, T. Lanz, Z. Kingsbury, M. Ross, B. Basu, R. Baird, D. J. Lomas, E. Sala, J. Watson, O. M. Rueda, S.-P. Chin, I. B. Wilkinson, M. J. Graves, J. E. Abraham, F. J. Gilbert, C. Caidas and K. M. Brindle, *Proc. Natl. Acad. Sci.*, **2020**, 117, 2092-2098.

[5] S. J. Elliott, Q. Stern, M. Ceillier, T. El Daraï, S. F. Cousin, O. Cala and S. Jannin, *Prog. Nucl. Magn. Reson. Spectrosc.*, **2021**, 126-127, 59-100.

[6] J. M. O. Vinther, V. Zhurbenko, M. M. Albannay and J. H. Ardenkjær-Larsen, *Solid State Nucl. Magn. Reson.*, **2019**, 102, 12-20.

[7] G. Hartmann, D. Hubert, S. Mango, C. C. Morehouse and K. Plog, *Nucl. Instrum. Meth. A*, **1973**, 106, 9-12.

[8] A. Bornet, R. Melzi, A. J. Perez Linde, P. Hautle, B. van den Brandt, S. Jannin and G. Bodenhausen, *J. Chem. Phys. Lett.*, **2013**, 4, 111-114.
[9] B. Vuichoud, A. Bornet, F. de Nanteuil, J. Milani, E. Canet, X. Ji, P. Miéville, E. Weber, D. Kurzbach, A. Flamm, R. Konrat, A. D. Gossert, S. Jannin and G. Bodenhausen, *Chem. Eur. J.*, **2016**, 22, 14696-14700.
[10] M. Cavaillès, A. Bornet, X. Jaurand, B. Vuichoud, D. Baudouin, M. Baudin, L. Veyre, G. Bodenhausen, J.-N. Dumez, S. Jannin, C. Copéret and C. Thieuleux, *Angew. Chem. Int. Ed.*, **2018**, 130, 7575-7579.
[11] S. R. Hartmann and E. L. Hahn, *Phys. Rev.*, **1962**, 128, 204-205.
[12] A. Pines, M. Gibby and J. Waugh, *Chem. Phys. Lett.*, **1972**, 15, 373-376.
[13] S. Jannin, A. Bornet, S. Colombo and G. Bodenhausen, *Chem. Phys. Lett.*, **2011**, 517, 234-236.
[14] A. Bornet, R. Melzi, S. Jannin and G. Bodenhausen, *Appl. Magn. Reson.*, **2012**, 43, 107-117.
[15] M. Batel, M. Krajewski, A. Däpp, A. Hunkeler, B. H. Meier, S. Kozerke and M. Ernst, *Chem. Phys. Lett.*, **2012**, 554, 72-76.
[16] X. Ji, A. Bornet, B. Vuichoud, J. Milani, D. Gajan, A. J. Rossini, L. Emsley, G. Bodenhausen and S. Jannin, *Nat. Commun*., **2017**, 8, 13975.
[17] T. El Daraï, S. F. Cousin, Q. Stern, M. Ceillier, J. G. Kempf, D. Eshchenko, R. Melzi, M. Schnell, L. Gremillard, A. Bornet, J. Milani, B. Vuichoud, O. Cala, D. Montarnal and S. Jannin, *Nat. Commun*., **2021**, 12, 4695.
[18] K. W. Lipsø, S. Bowen, O. Rybalko and J. H. Ardenkjær-Larsen, *J. Magn. Reson.*, **2017**, 274, 65-72.
[19] S. J. Elliott, S. F. Cousin, Q. Chappuis, O. Cala, M. Ceillier, A. Bornet and S. Jannin, *Magn. Reson.*, **2020**, 1, 89-96.
[20] J. Jeener, R. Du Bois and P. Broekaert, *Phys. Rev.*, **1965**, 139, A1959-A1961.
[21] J. Jeener and P. Broekaert, *Phys. Rev.*, **1967**, 157, 232-240.
[22] A. G. Redfield, *Science*, **1969**, 164, 1015-1023.
[23] S. Emid, J. Konijnendijk, J. Smidt and A. Pines, *Physica B+C*, **1980**, 100, 215-218.
[24] H.-M. Vieth and C. S. Yannoni, *Chem. Phys. Lett.*, **1993**, 205, 153-156.
[25] N. D. Kurur and G. Bodenhausen, *J. Magn. Reson. A*, **1995**, 114, 163-173.
[26] J.-S. Lee and A. K. Khitrin, *J. Magn. Reson.*, **2005**, 177, 152-154.
[27] R. Ohasi, K. Takegoshi and T. Terao, *Solid State Nucl. Magn. Reson.*, **2007**, 31, 115-118.
[28] J.-S. Lee and A. K. Khitrin, *J. Chem. Phys.*, **2008**, 128, 114504.
[29] A. K. Khitrin, J. Xu and A. Ramamoorthy, *J. Magn. Reson.*, **2011**, 212, 95-101.
[30] J. D. van Beek, A. Hemmi, M. Ernst and B. H. Meier, *J. Chem. Phys.*, **2011**, 135, 154507.
[31] H. Jóhannesson, S. Macholl and J. H. Ardenkjær-Larsen, *J. Magn. Reson.*, **2009**, 197, 167-175.
[32] B. Vuichoud, J. Milani, A. Bornet, R. Melzi, S. Jannin and G. Bodenhausen, *J. Phys. Chem. B*, **2014**, 118, 1411-1415.
[33] A. Bornet, J. Milani, B. Vuichoud, A. J. Perez Linde, G. Bodenhausen and S. Jannin, *Chem. Phys. Lett.*, **2014**, 602, 63-67.
[34] S. J. Elliott, Q. Stern and S. Jannin, Solid-State ^{1}H Spin Polarimetry by $^{13}CH_3$ Nuclear Magnetic Resonance, *Accepted in Magn. Reson.*, **2021**, https://doi.org/10.5194/mr-2021-25.
[35] A. Bornet, A. C. Pinon, A. Jhajharia, M. Baudin, X. Ji, L. Emsley, G. Bodenhausen, J. H. Ardenkjær-Larsen and S. Jannin, *Phys. Chem. Chem. Phys.*, **2016**, 18, 30530-30535.
[36] S. J. Elliott, O. Cala, Q. Stern, S. F. Cousin, D. Eshchenko, R. Melzi, J. G. Kempf and S. Jannin, *Phys. Chem. Chem. Phys.*, **2021**, 23, 9457-9465.
[37] S. J. Elliott et al., *Accepted in J. Magn. Reson. Open*, **2021**, https://doi.org/10.1016/j.jmro.2021.100018.
[38] X.-A. Mao and C.-H. Ye, *Concept Magn. Reson. A*, **1998**, 9, 173-187.
[39] V. V. Krishnan and N. Murali, *Prog. Nucl. Magn. Reson. Spectrosc.,* **2013**, 68, 41-57.